Supplementary Materials: Low-Dimensional Compounds Containing Bioactive Ligands. Part XX: Crystal Structures, Cytotoxic, Antimicrobial Activities and DNA/BSA Binding of Oligonuclear Zinc Complexes with Halogen Derivatives of 8-Hydroxyquinoline

Michaela Harmošová, Martin Kello, Michal Goga, Ľudmila Tkáčiková, Mária Vilková, Danica Sabolová, Simona Sovová, Erika Samoľová, Miroslava Litecká, Veronika Kuchárová, Juraj Kuchár and Ivan Potočňák

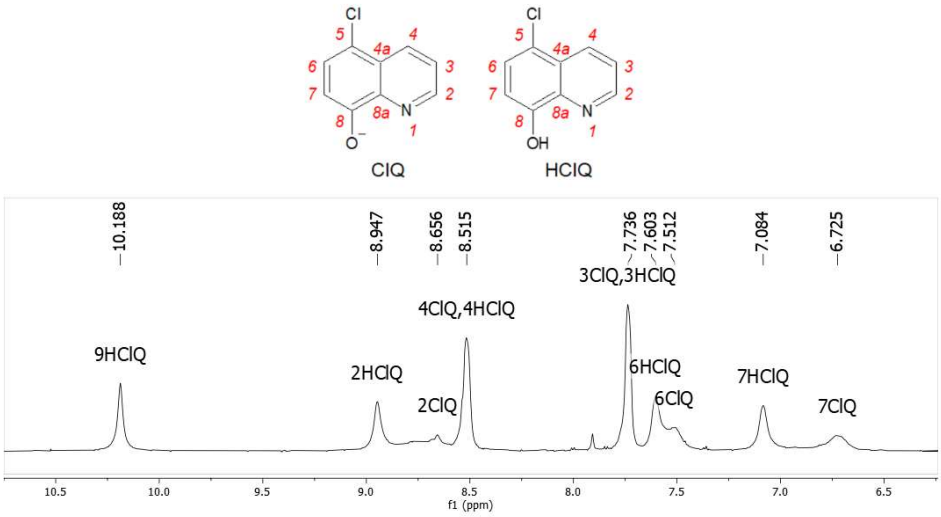

Figure S1. ^{1}H NMR (600 MHz, DMSO-d_6) spectrum of complex **3**.

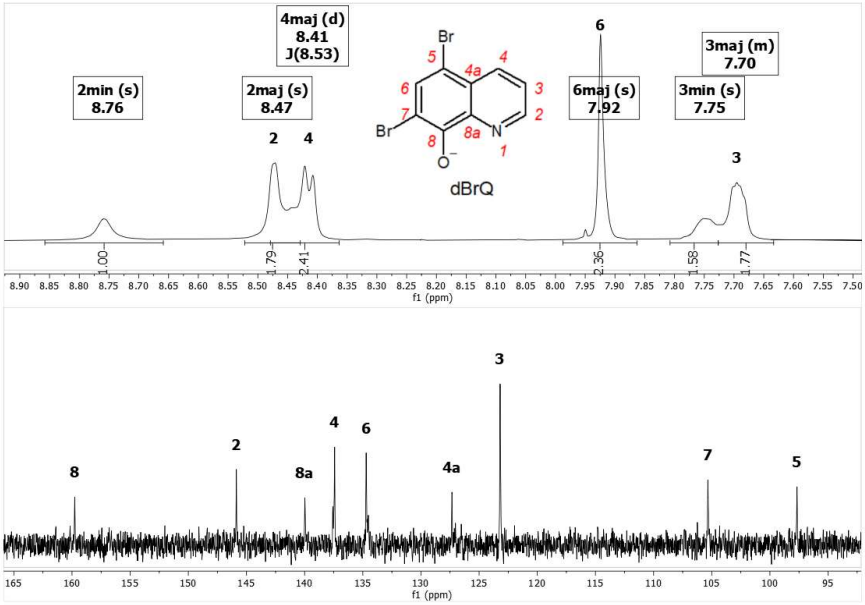

Figure S2. ^{1}H (600 MHz, DMSO-d$_6$) and ^{13}C (150 MHz, DMSO-d$_6$) NMR spectrum of complex **5**.

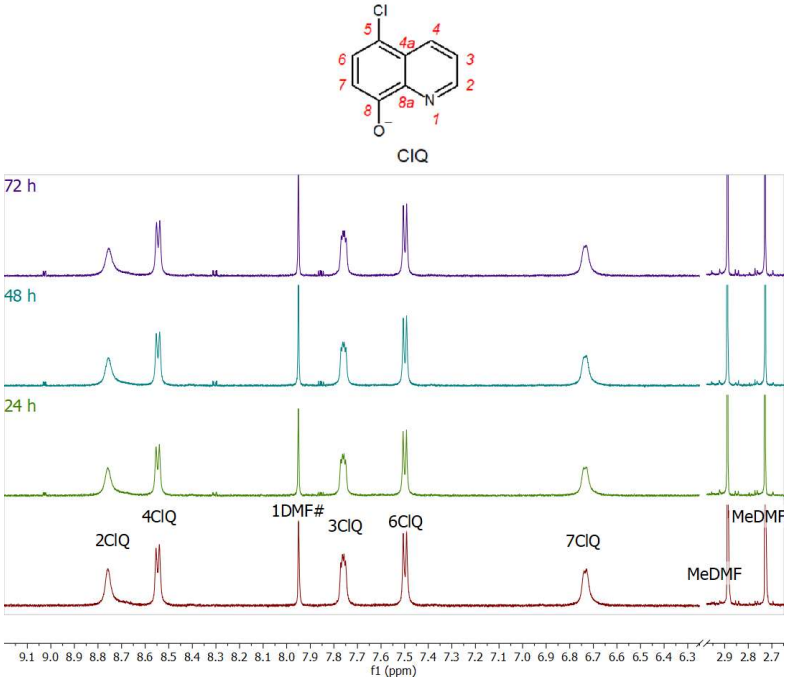

Figure S3. Time-dependent ^{1}H NMR (600 MHz, DMSO-d$_6$) spectra of complex **2**.

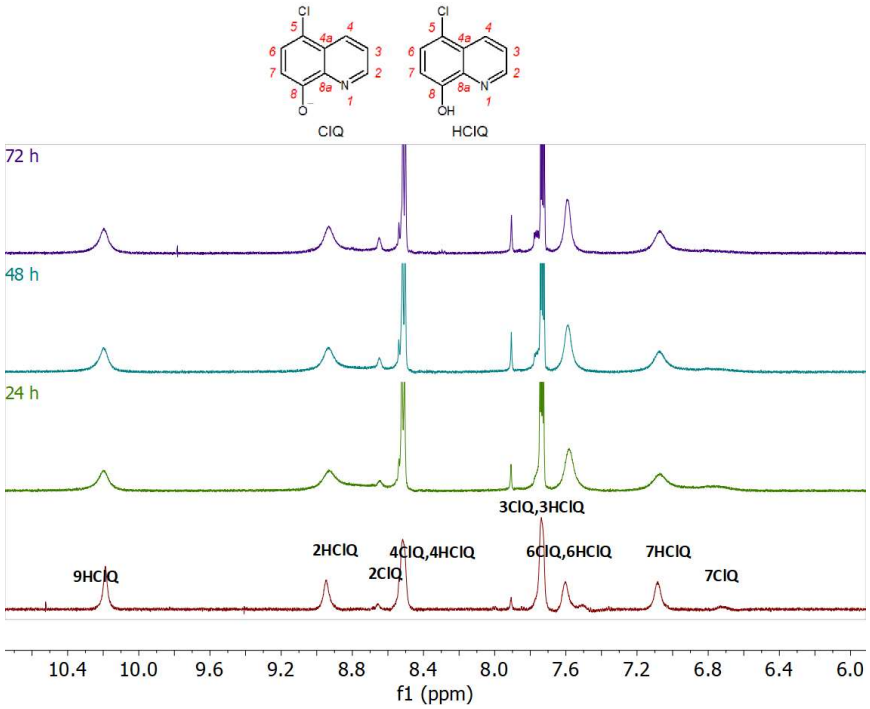

Figure S4. Time-dependent ^{1}H NMR (600 MHz, DMSO-d_6) spectra of complex **3**.

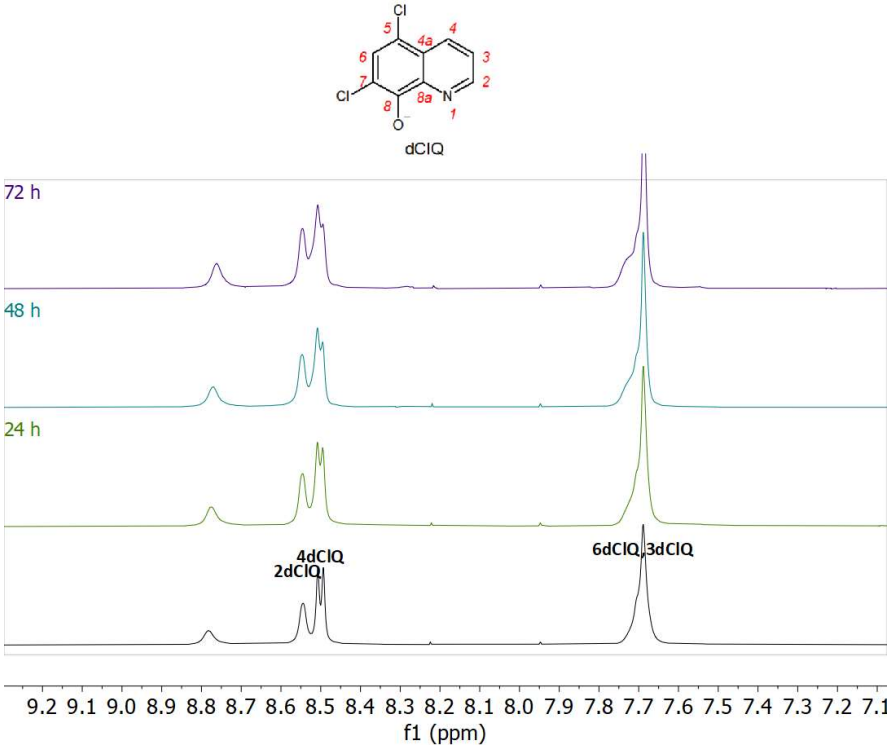

Figure S5. Time-dependent ^{1}H NMR (600 MHz, DMSO-d_6) spectra of complex **4**.

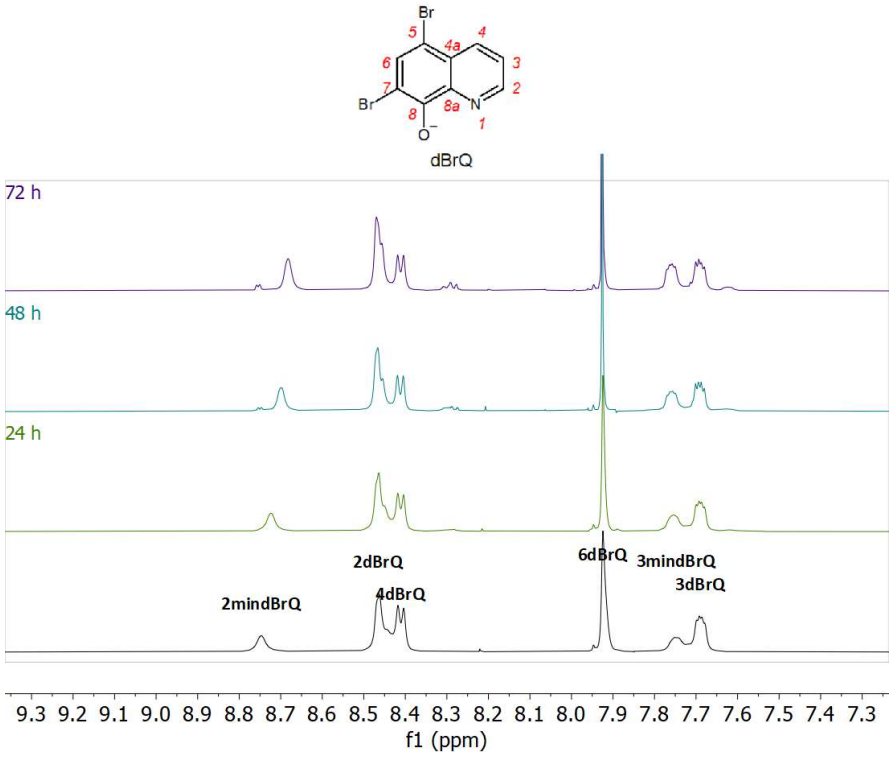

Figure S6. Time-dependent ^{1}H NMR (600 MHz, DMSO-d$_6$) spectra of complex **5**.

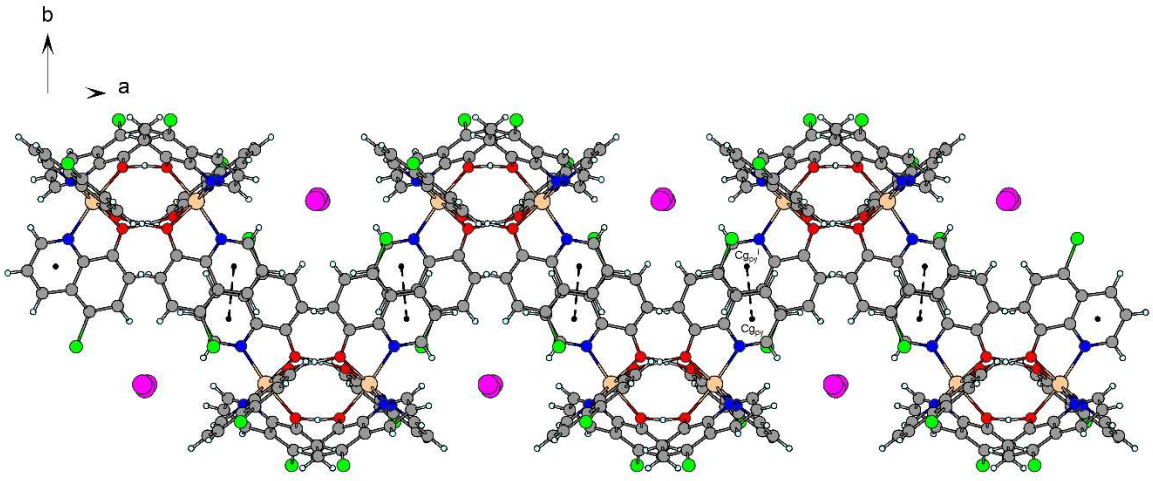

Figure S7. Part of the one-dimensional structure of **3** viewed along the *c* axis with π-π interactions (black dashed lines).

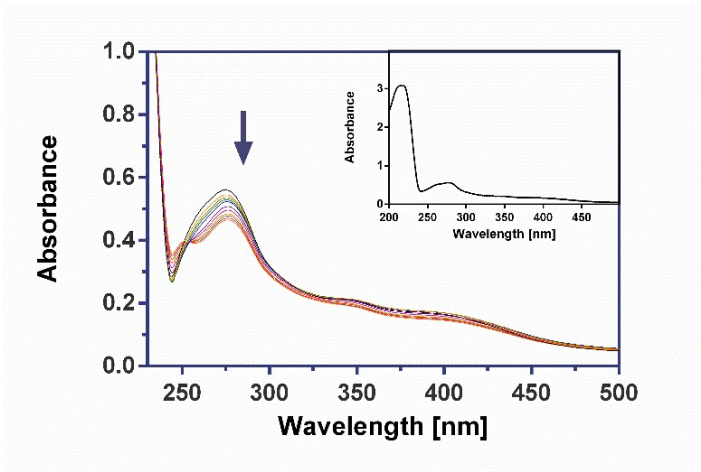

Figure S8. UV-vis spectrum of complex **1** (6.14×10^{-6} M) with ctDNA. The arrow indicates changes in absorbance upon increasing DNA concentration. Inset: UV-vis absorption spectrum of **1**.

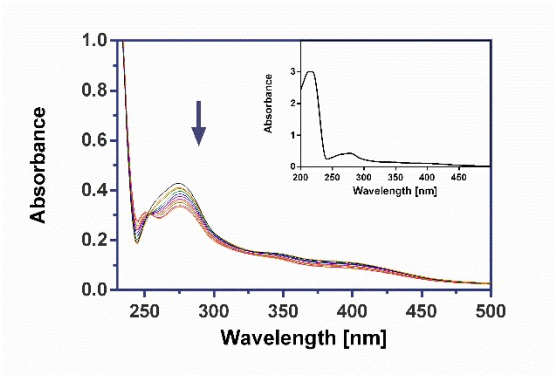

Figure S9. UV-vis spectrum of complex **2** (6.14×10^{-6} M) with ctDNA. The arrow indicates changes in absorbance upon increasing DNA concentration. Inset: UV-vis absorption spectrum of **2**.

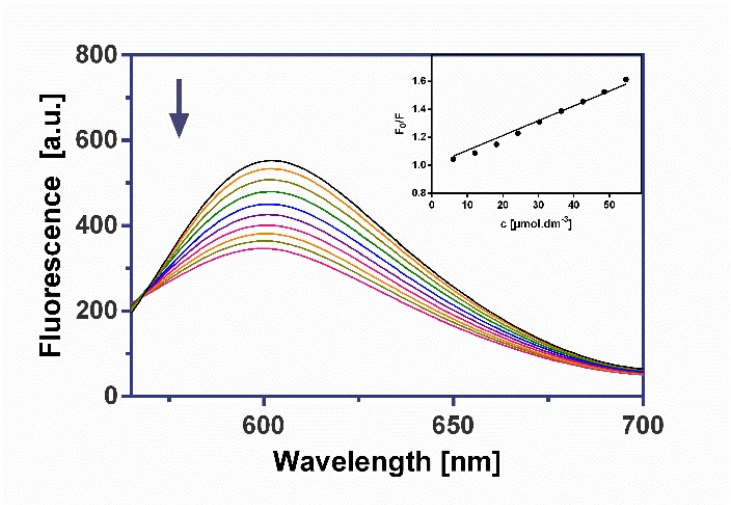

Figure S10. Fluorescence spectrum of DNA-EB complex in the absence (black line) and presence of complex **1.** Inset: The corresponding Stern-Volmer plot for quenching process of EB by **1.**

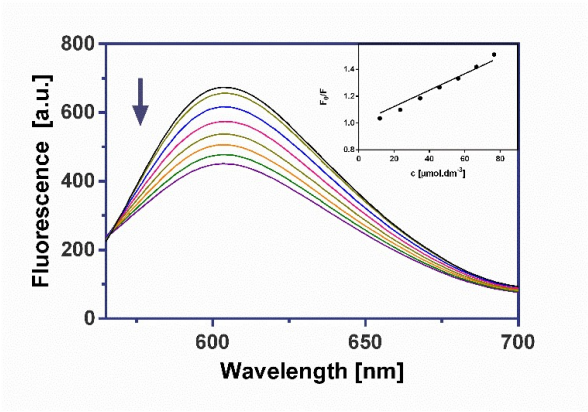

Figure S11. Fluorescence spectrum of DNA-EB complex in the absence (black line) and presence of complex **2.** Inset: The corresponding Stern-Volmer plot for quenching process of EB by **2.**

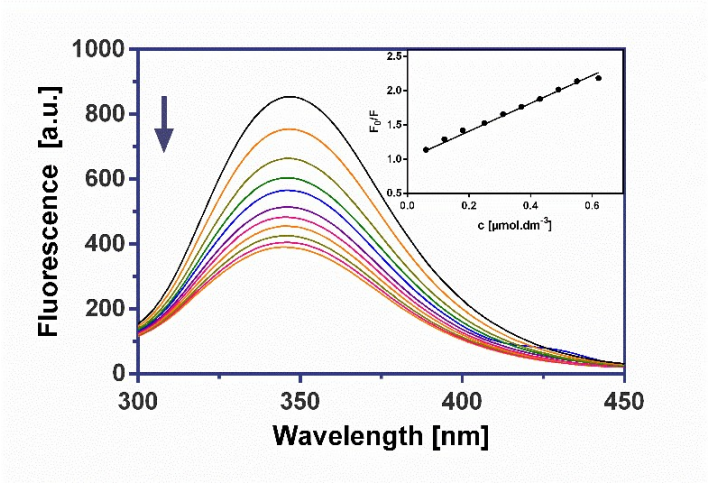

Figure S12. Fluorescence quenching spectra of BSA in presence of complex **1**. Inset: The corresponding Stern-Volmer plot for **1** at 25 °C.

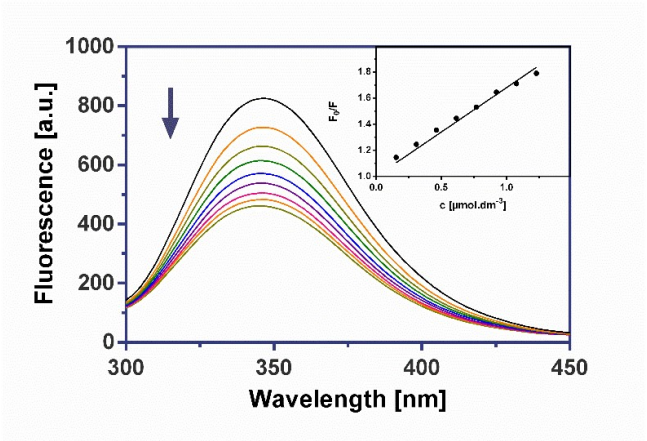

Figure S13. Fluorescence quenching spectra of BSA in presence of complex **2**. Inset: The corresponding Stern-Volmer plot for **2** at 25 °C.

Table S1. ^{13}C NMR (150 MHz, DMSO-d6) chemical shifts δC [ppm] for complexes **1** – **5**.

		δC								
		C-2	**C-3**	**C-4**	**C-4a**	**C-5**	**C-6**	**C-7**	**C-8**	**C-8a**
1*	ClQ	145.6	122.8	135.0	126.6	108.9	130.0	111.6	162.3	139.7
2*	ClQ	145.7	122.8	135.0	126.6	109.0	130.0	111.7	162.3	140.2
3										
4**	dClQ	146.1 147.0	122.7	135.1	125.7 125.4	108.5	129.5	114.8	158.2 157.2	140.0 139.6
5**	dBrQ	145.9	123.2	137.4 137.6	127.3	97.7	134.7 134.6	105.3	159.8	140.0

*162.3 (C=ODMF), 35.8 (MeDMF), 30.8 (MeDMF)

**chemical shifts for major form are in the first line and for the minor form in the second line

Table S2. Data describing different polyhedral distortions for **1** – **5**.

Complex	Σ [a]	CShM [b]	τ	CShM [c]	CShM [d]
1	121.32	2.968	0.6953	3.083	4.070
2	101.34	2.407	0.0843	4.314	1.030
3	88.48	1.594			
4	53.6	0.708			
5	(Zn1) 54	0.761			
	(Zn2)57.3	0.977			

[a] octahedral distortion parameter $\Sigma = (|90 - \varphi_i|)$ [$\Sigma = 0°$ for an ideal octahedron; φ_i represents the twelve smallest L–M–L angles]

[b] CShM represents result from continuous shape measures of donor atoms positions relative to the vertices of an ideal octahedron

[c] CShM represents result from continuous shape measures of donor atoms positions relative to the vertices of an ideal trigonal bipyramid

[d] CShM represents result from continuous shape measures of donor atoms positions relative to the vertices of an ideal spherical square pyramid

Table S3. Cg···Cg distances and angles (Å, °) characterizing π-π interactions in **1** and **2**.

Complex	Cg(I)···Cg(J) [a]	Cg···Cg	α [b]	β	γ
1	Cg_{py1}···Cg_{ph1}^{i}	3.4821(15)	18.69(13)	14.2	5.2
2	Cg_{py1}···Cg_{py2}^{i}	3.5821(1)	7.16(9)	17.2	15.6
	Cg_{ph1}···Cg_{ph2}^{i}	3.6236(1)	8.81(9)	14.1	16.5

[Symmetry codes: (i) = -*x*+1, -*y*+1, -*z*+1 (**1**), (**2**)]

[a]Cg_{py1} represents centroid of the pyridine ring containing N1 atom

Cg_{py2} represents centroid of the pyridine ring containing N2 atom

Cg_{ph1} represents centroid of the phenyl ring containing C18 atom

Cg_{ph2} represents centroid of the phenyl ring containing C28 atom

[b] α is the dihedral angle between planes I and J. β is the angle between Cg(I)···Cg(J) vector and normal to plane I. γ is the angle between Cg(I)···Cg(J) vector and normal to plane J

Table S4. Cg···Cg distances and angles (Å, °) characterizing π-π interactions in **3**.

Cg(I)···Cg(J) [a]	Cg···Cg	α [b]	β	γ
Cg_{py}···Cg_{py}^{i}	3.7466	0	29.4	29.4

[Symmetry code: (i) = -*x*+1.5, -*y*+2.5, -*z*+1.5]

[a] Cg_{py} represents centroid of the pyridine ring containing N2 atom

[b] α is the dihedral angle between planes I and J. β is the angle between Cg(I)···Cg(J) vector and normal to plane I. γ is the angle between Cg(I)···Cg(J) vector and normal to plane

Table S5. Cg···Cg distances and angles (Å, °) characterizing π-π interactions in **5**.

Cg(I)···Cg(J) [a]	Cg···Cg	α [b]	β	γ
Cg_{ph1}···Cg_{ph6}^{i}	3.773(5)	1.4	20.7	20.2
Cg_{ph1}···Cg_{ph6}^{ii}	3.792(5)	1.4	17.8	18.4

[Symmetry codes: (i) = 1-*x*, 1-*y*, 1-*z*; (ii) = 2-*x*, 1-*y*, 1-*z*]

[a] Cg_{ph1} represents centroid of the carbocyclic ring containing C18 atom

Cg_{ph6} represents centroid of the carbocyclic ring containing C68 atom

[b] α is the dihedral angle between planes I and J. β is the angle between Cg(I)···Cg(J) vector and normal to plane I. γ is the angle between Cg(I)···Cg(J) vector and normal to plane J